Systematic study of the α decay preformation factors of the nuclei around the $Z = 82$, $N = 126$ shell closures within the generalized liquid drop model *

Hong-Ming Liu(刘宏铭)[1] You-Tian Zou(邹有甜)[1] Xiao Pan(潘霄)[1]
Xiao-Jun Bao(包小军)[2,4;1)] Xiao-Hua Li(李小华)[1,3,4;2)]

[1]School of Nuclear Science and Technology, University of South China, Hengyang 421001, China
[2]Hunan Normal University, Changsha 410081, China
[3]Cooperative Innovation Center for Nuclear Fuel Cycle Technology & Equipment, University of South China, Hengyang 421001, China
[4]Key Laboratory of Low Dimensional Quantum Structures and Quantum Control, Hunan Normal University, Changsha 410081, China

Abstract: In this study, we systematically investigate the α decay preformation factors, P_α, and the α decay half-lives of 152 nuclei around $Z = 82$, $N = 126$ closed shells based on the generalized liquid drop model (GLDM) with P_α being extracted from the ratio of the calculated α decay half-life to the experimental one. The results show that there is a remarkable linear relationship between P_α and the product of valance protons (holes) N_p and valance neutrons (holes) N_n. At the same time, we extract the α decay preformation factor values of the even–even nuclei around the $Z = 82$, $N = 126$ closed shells from the study of Sun *et al.* [J. Phys. G: Nucl. Part. Phys., **45**: 075106 (2018)], in which the α decay was calculated by two different microscopic formulas. We find that the α decay preformation factors are also related to N_pN_n. Combining with our previous studies [Sun *et al.*, Phys. Rev. C, **94**: 024338 (2016); Deng *et al.*, ibid. **96**: 024318 (2017); Deng *et al.*, ibid. **97**: 044322 (2018)] and that of Seif *et al.*, [Phys. Rev. C, **84**: 064608 (2011)], we suspect that this phenomenon of linear relationship for the nuclei around the above closed shells is model-independent. This may be caused by the effect of the valence protons (holes) and valence neutrons (holes) around the shell closures. Finally, using the formula obtained by fitting the α decay preformation factor data calculated by the GLDM, we calculate the α decay half-lives of these nuclei. The calculated results agree with the experimental data well.

Keywords: α decay, α decay preformation factor, shell closure, generalized liquid drop model

DOI: 10.1088/1674-1137/44/9/094106

1 Introduction

α decay, which is one of the most significant tools for exploring nuclear structure information, can provide information of the ground-state lifetime, nuclear force, nuclear matter incompressibility, and spin and parity of nuclei [1-4]. In 1928, Gamow, Condon, and Gurney independently proposed the quantum tunneling theory [5, 6], named as Gamow theory. Within this theory, the α decay is explained as an α cluster preformed in the surface of the parent nucleus penetrating the Coulomb barrier between the cluster and the daughter nucleus. The probability of α cluster formation in the parent nucleus is described as the α preformation factor, P_α, including many nuclear structure information. It has became a prominent topic in nuclear physics [7-10].

Until now, many microscopical and phenomenological models have been used to calculate P_α [11-25]. Microscopically, in the R-matrix method [11-15], P_α can be obtained by the initial tailored wavefunction of the parent nucleus. However, the calculation of purely microcosmic

Received 8 February 2020, Published online 27 July 2020

* Supported in part by the National Natural Science Foundation of China (11205083, 11505100, 11705055), the Construct Program of the Key Discipline in Hunan Province, the Research Foundation of Education Bureau of Hunan Province, China (15A159, 18A237), the Natural Science Foundation of Hunan Province, China (2015JJ3103, 2015JJ2121, 2018JJ3324), the Innovation Group of Nuclear and Particle Physics in USC, the Shandong Province Natural Science Foundation, China (ZR2015AQ007), the Hunan Provincial Innovation Foundation For Postgraduate (CX20190714, CX20200909), the National Innovation Training Foundation of China (201910555161), and the Opening Project of Cooperative Innovation Center for Nuclear Fuel Cycle Technology and Equipment, University of South China (2019KFZ10)

1) E-mail: baoxiaojun@hunnu.edu.cn
2) E-mail: lixiaohuaphysics@126.com

P_α is very difficult owing to the complexity of the nuclear many-body problem and the uncertainty of the nuclear potential. The α preformation factors can also obtained by the approach of the microscopical Tohsaki–Horiuchi–Schuck–Röpke wave function [16, 17], which has been successfully employed to describe the cluster structure in light nuclei [17]. Using the cluster-configuration shell model, Varga *et al*. reproduced the experimental decay width of ^{212}Po and obtained its α preformation factor P_α = 0.23 [11, 15]. Recently, Ahmed *et al*. proposed a new quantum-mechanical theory named as cluster-formation model (CFM) to calculate the α preformation factors, P_α, of even–even nuclei [19, 26]. Within this model, P_α can be obtained from the ratio of the formation energy, $E_{f\alpha}$, to the total energy, E, where $E_{f\alpha}$ and E can be obtained from the binding energies of the nucleus and its neighboring nuclides. Later, Deng *et al*. and Ahmed *et al*. extended this model to odd-A and odd–odd nuclei [20-22]. Generally, within different theoretical models, the α preformation factors, P_α are different because the penetration probability varies greatly with an exponential factor. Phenomenologically, the preformation factors, P_α, are extracted from the ratios of the calculated α decay half-lives to the experimental ones [23-25]. In 2005, using the density-dependent cluster model (DDCM) [18], Xu and Ren studied the available experimental α decay half-lives of medium-mass nuclei. Their results showed that the P_α are different for different types of parent nuclei, i.e., P_α = 0.43 for even–even nuclei, 0.35 for odd-A nuclei, and 0.18 for doubly odd nuclei.

Recent studies have been shown that the α preformation factors are affected by many confirmed factors, such as the isospin asymmetry of the parent nucleus, deformation of the daughter, pairing effect, and shell effect [9, 27]. It has been observed that the minima of the α preformation factors are at the protons, neutron shells, and subshell closures [8, 9, 28-31]. Moreover, many nuclear quantities [32-36], such as deformation and B (E2) values [32, 33], rotational moments of inertia in low-spin states in the rare earth region [34], core cluster decomposition in the rare-earth region [35], and properties of excited states [36], display a systematic behavior with the product of valence protons (holes) N_p and valence neutrons (holes) N_n of the parent nucleus. In 2011, Seif *et al.* found that the α preformation factor is linearly proportional to the product of N_p and N_n for even–even nuclei around Z = 82 and N = 126 closed shells [37]. In our previous studies [38-40], based on the two-potential approach (TPA) [41, 42], we found that this linear relationship also exists in the cases of odd-A and doubly-odd nuclei for favored and unfavored α decay [38, 39]. Very recently, using the CFM, we calculated the α preformation factors of all kinds of nuclei and found that this linear relationship also existed in these cases [40]. Combined with the study of Seif *et al.* and our previous studies, it is interesting to validate whether this linear relationship is model-dependent or owing to the valence proton–neutron interaction of the shell closures. In the present study, using the generalized liquid drop model (GLDM) [43-49], we systematically study the α preformation factors, P_α, and α decay half-lives of 152 nuclei around Z = 82, N = 126 shell closures. Our results show that the α preformation factors of these nuclei and N_pN_n still satisfy this linear relationship, which suggests that this relationship may be owing to the valence proton–neutron correlation around Z = 82, N = 126 shell closures.

This article is organized as follows. In the next section, the theoretical framework of the GLDM is briefly presented. The detailed calculations and discussion are presented in Section 3. Finally, a summary is given in Section 4.

2 Theoretical framework

The α decay half-life can be calculated by decay constant λ, which can be written as

$$T_{1/2} = \frac{\ln 2}{\lambda}. \tag{1}$$

Here, the α decay constant is defined as

$$\lambda = P_\alpha \nu P, \tag{2}$$

where P_α is the α preformation factor. P, the penetration probability of the α particle crossing the barrier, is calculated by Eq. (12) expressed subsequently. ν is the assault frequency, which can be calculated with the oscillation frequency, ω, and is written as [50]

$$\nu = \frac{\omega}{2\pi} = \frac{(2n_r + l + \frac{3}{2})\hbar}{2\pi\mu {R_n}^2} = \frac{(G + \frac{3}{2})\hbar}{1.2\pi\mu {R_{00}}^2}, \tag{3}$$

where $\mu = \frac{m_d m_\alpha}{m_d + m_\alpha}$ represents the reduced mass between the α particle and the daughter nucleus with m_d and m_α being the masses of the daughter nucleus and α particle, respectively. $\hbar$ is the reduced Planck constant. $R_n = \sqrt{\frac{3}{5}} R_{00}$ denotes the nucleus root-mean-square (rms) radius with $R_{00} = 1.240A^{1/3}\left(1 + \frac{1.646}{A} - 0.191\frac{A-2Z}{A}\right)$ [51], where A and Z are the proton and mass numbers of the parent nucleus. $G = 2n_r + l$ represents the main quantum number with n_r and l being the radial quantum number and the angular quantity quantum number, respectively. For the α decay, G can be obtained by [52]

$$G = 2n_r + l = \begin{cases} 18, & N \leqslant 82, \\ 20, & 82 < N \leqslant 126, \\ 22, & N < 126. \end{cases} \tag{4}$$

$l_{\min}$, the minimum angular momentum taken away by the α particle, can be obtained by [53]

$$l_{\min}=\begin{cases}\Delta_j, & \text{for even } \Delta_j \text{ and } \pi_p=\pi_d,\\ \Delta_j+1, & \text{for even } \Delta_j \text{ and } \pi_p\neq\pi_d,\\ \Delta_j, & \text{for odd } \Delta_j \text{ and } \pi_p\neq\pi_d,\\ \Delta_j+1, & \text{for odd } \Delta_j \text{ and } \pi_p=\pi_d,\end{cases} \tag{5}$$

where $\Delta_j=\left|j_p-j_d\right|$. j_p, π_p, j_d, π_d represent the spin and parity values of the parent and daughter nuclei, respectively.

The GLDM has been successfully employed to describe fusion reactions [47] and nuclear decays [46, 48, 49]. Within the GLDM, the macroscopic total energy, E, is defined as [44]

$$E=E_{\rm S}+E_{\rm V}+E_{\rm C}+E_{\rm prox}, \tag{6}$$

where $E_{\rm S}$, $E_{\rm V}$, $E_{\rm C}$, and $E_{\rm prox}$ are the surface, volume, Coulomb, and proximity energies, respectively. For one-body shapes, $E_{\rm S}$, $E_{\rm V}$, and $E_{\rm C}$ can be expressed as

$$\begin{aligned}E_{\rm S}&=17.9439(1-2.6I^2)A^{2/3}(S/4\pi R_0^2)\,{\rm MeV},\\ E_{\rm V}&=-15.494(1-1.8I^2)A\,{\rm MeV},\\ E_{\rm C}&=0.6e^2(Z^2/R_0)\times 0.5\int(V(\theta)/V_0)(R(\theta)/R_0)^3\sin\theta\,{\rm d}\theta,\end{aligned} \tag{7}$$

where $I=(N-Z)/A$ is the relative neutron excess. S is the surface of the deformed nucleus. $V(\theta)$ is the electrostatic potential at the surface, and V_0 is the surface potential of the sphere. $R_0=1.28A^{1/3}-0.76+0.8A^{-1/3}$ is the effective sharp radius [43].

For two separated spherical nuclei, the $E_{\rm S}$, $E_{\rm V}$, and $E_{\rm C}$ are defined as

$$\begin{aligned}E_{\rm S}&=17.9439[(1-2.6{I_1}^2){A_1}^{2/3}+(1-2.6{I_2}^2){A_2}^{2/3}]\,{\rm MeV},\\ E_{\rm V}&=-15.494[(1-1.8{I_1}^2)A_1+(1-1.8{I_2}^2)A_2]\,{\rm MeV},\\ E_{\rm C}&=0.6e^2{Z_1}^2/R_1+0.6e^2{Z_2}^2/R_2+e^2Z_1Z_2/r\,{\rm MeV},\end{aligned} \tag{8}$$

where A_i, Z_i, and I_i are the mass number, charge number, and relative neutron excesses of these nuclei, respectively. r is the distance between the mass centers. R_1 and R_2 are the radii of the daughter nuclei and the α particle, respectively, which can obtained by the following relationships:

$$\begin{aligned}R_1&=R_0(1+\beta^3)^{-1/3},\\ R_2&=R_0\beta(1+\beta^3)^{-1/3},\end{aligned} \tag{9}$$

where

$$\beta=\frac{1.28{A_2}^{1/3}-0.76+0.8{A_2}^{-1/3}}{1.28{A_1}^{1/3}-0.76+0.8{A_1}^{-1/3}}. \tag{10}$$

The surface energy, $E_{\rm S}$, originates from the effects of the surface tension forces in a half-space and does not include the contribution of the attractive nuclear forces between the considered surfaces in the neck or in the gap between the fragments. The nuclear proximity energy term, $E_{\rm prox}$, has been introduced to take into account these additional surface effects. It can be defined as

$$E_{\rm prox}(r)=2\gamma\int_{h_{\min}}^{h_{\max}}\Phi[D(r,h)/b]2\pi h\,{\rm d}h. \tag{11}$$

Here, h is the transverse distance varying from the neck radius or zero to the height of the neck border. After the separation, $h_{\min}=0$ and $h_{\max}=R_2$. D is the distance between the opposite infinitesimal surfaces considered, b is the surface width fixed at the standard value of 0.99 fm, Φ is the proximity function of Feldmeier, and $\gamma=0.9517\sqrt{(1-2.6{I_1}^2)(1-2.6{I_2}^2)}$ MeVfm^{-2} is the geometric mean between the surface parameters of the two nuclei.

P, the penetration probability of the α particle crossing the barrier, is calculated within the action integral as follows:

$$P=\exp\left[-\frac{2}{\hbar}\int_{R_{\rm in}}^{R_{\rm out}}\sqrt{2B(r)(E(r)-E({\rm sphere}))}\,{\rm d}r\right]. \tag{12}$$

Here, $B(r)=\mu$, Q_α is the α decay energy, and $R_{\rm in}$ and $R_{\rm out}$ are the two turning points of the semiclassical Wentzel–Kramers–Brillouin (WKB) action integral with $E(R_{\rm in})=E(R_{\rm out})=Q_\alpha$. $R_{\rm in}=R_1+R_2$. Consisdering the contribution of the centrifugal potential, $R_{\rm out}$ can be obtained by

$$R_{\rm out}=\frac{Z_1Z_2e^2}{2Q_\alpha}+\sqrt{\left(\frac{Z_1Z_2e^2}{2Q_\alpha}\right)^2+\frac{l(l+1)\hbar^2}{2\mu Q_\alpha}}. \tag{13}$$

3 Results and discussion

In recent years, many studies have indicated that the α preformation factor, P_α, of a nucleus becomes smaller as the valence nucleus (hole) becomes smaller [23-25]. Meanwhile, intensive studies related to the N_pN_n scheme have indicated the importance of the proton–neutron interaction in determining the evolution of the nuclear structure [54-58]. In 2011, Seif *et al.* found that the P_α are linearly related to the product of the valence proton numbers and the valence neutron numbers, N_pN_n, for even–even nuclei around $Z=82$, $N=126$ shell closures [37]. Very recently, we found that this linear relationship still exists in the cases of odd-A and doubly-odd nuclei for favored and unfavored α decays [38-40]. Moreover, we systematically studied the P_α based on the CFM [19-22] of all kinds of nuclei around $Z=82$, $N=126$ shell closures. The results indicated that the linear relationship between the α preformation factors and N_pN_n still exists. Whether this phenomenon is model-dependent or may be the effect of the valance proton –neutron interaction around the closed shells is an interesting problem. In the

present study, we use the GLDM to systematically study the P_α and α decay half-lives of the nuclei around $Z = 82$, $N = 126$ shell closures, with the experimental α decay half-lives, $T_{1/2}^{\rm expt}$, being taken from the latest evaluated nuclear properties table, NUBASE2016 [59].

First, we calculate the α preformation factors, P_α, of 152 nuclei (including 47 even–even nuclei, 73 odd-A nuclei, and 32 doubly-odd nuclei) around the $Z = 82$, $N = 126$ shell closures through $P_\alpha = \dfrac{T_{1/2}^{\rm calc}}{T_{1/2}^{\rm expt}}$, whereas the theoretical calculations, $T_{1/2}^{\rm calc}$, are obtained by the GLDM. The calculated results of P_α are listed in the fifth columns of Tables 1–5. For more clearly observing the relationship between the obtained P_α and N_pN_n for these nuclei, we plot the P_α as a function of $\dfrac{N_pN_n}{Z_0+N_0}$ in five cases in Figs. 1–3 (Fig. 1 for the case of even–even nuclei, Fig. 2 for the cases of the favored and unfavored odd-A nuclei, and Fig. 3 for the cases of the favored and unfavored doubly-odd nuclei). To more clearly describe N_p and N_n bounded by the double magic numbers of $Z = 82$ and $N = 126$, we divide these 152 nuclei into three regions. In region I, the proton number of a nucleus is above the $Z = 82$ shell closure and the neutron number is below the $N = 126$ closed shell and the $\dfrac{N_pN_n}{Z_0+N_0}$ value is negative. In region II, the proton number of a nucleus is above the $Z = 82$ shell closure and the neutron number is above the $N = 126$ closed shell and the $\dfrac{N_pN_n}{Z_0+N_0}$ value is positive. In region III, the proton number of a nucleus is below the $Z = 82$ shell closure and the neutron number is above the $N = 126$ closed shell and the $\dfrac{N_pN_n}{Z_0+N_0}$ value is positive. In Fig. 1, the red dots represent the case of even–even nuclei α decay and the red dashed line represents the fittings of P_α for the cases of even–even nuclei α decay. In Figs. 2 and 3 the red dots and blue triangle represent the cases of the favored and unfavored α decays, respectively. The red dashed and blue solid lines represent the fittings of P_α. As we can see in Figs. 1–3, around the $Z = 82$, $N = 126$ shell closures, when the values of $\dfrac{N_pN_n}{Z_0+N_0}$ are positive, P_α increases basically with the increase of $\dfrac{N_pN_n}{Z_0+N_0}$. Similarly, when the values of $\dfrac{N_pN_n}{Z_0+N_0}$ are negative, P_α increases basically with the increase in $\dfrac{N_pN_n}{Z_0+N_0}$. Furthermore, we find that the linear relationships in Figs. 1-3 are relatively remarkable, except in the right sides of Figs. 2 and 3 for the cases of favored decay. Notably, some red

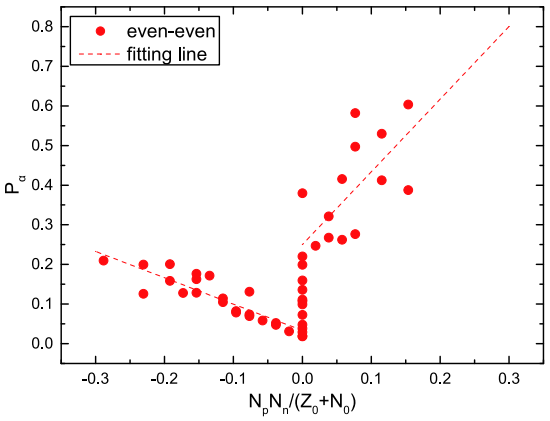

Fig. 1. (color online) α preformation factors of the even–even nuclei around the $Z_0 = 82$ and $N_0 = 126$ shell closures as a function of $\dfrac{N_pN_n}{N_0+Z_0}$, where N_p and N_n denote the numbers of valence protons (holes) and neutrons (holes) of the parent nucleus, respectively. The dashed lines are the fittings of the α preformation factors.

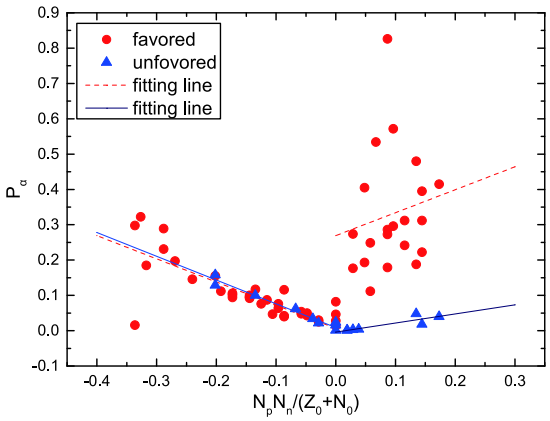

Fig. 2. (color online) Same as Fig. 1, but it represents the α preformation factors as a function of $\dfrac{N_pN_n}{N_0+Z_0}$ of the odd-A nuclei.

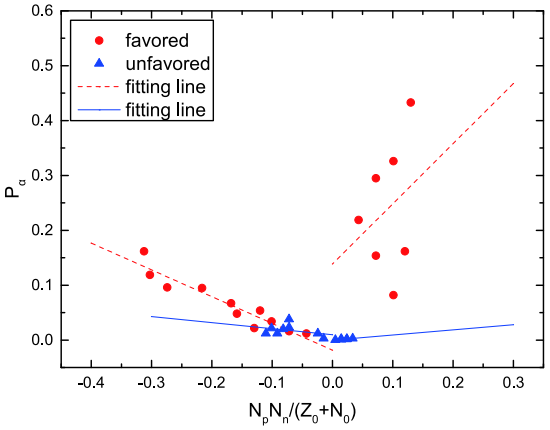

Fig. 3. (color online) Same as Fig. 1, but it represents the α preformation factors as a function of $\dfrac{N_pN_n}{N_0+Z_0}$ of the doubly-odd nuclei.

Table 1. Calculations of the α decay half-lives in logarithmic form and the α preformation factors of the even–even nuclei in regions I–III around the Z = 82, N = 126 closed shells. The experimental α decay half-lives, spin, and parity are taken from the latest evaluated nuclear properties table, NUBASE2016 [59]. The α decay energies, Q_α , are taken from the latest evaluated atomic mass table, AME2016 [60, 61]. The α preformation factors, P_α, are extracted from the ratios of the calculated α decay half-lives to the experimental data [23-25], where the calculated α decay half-lives are obtained by the GLDM.

α transition	Q_α/MeV	$J_p^\pi \to J_d^\pi$	$l_{\min}$	P_α	$\lg T_{1/2}^{\rm expt}$/s	$\lg T_{1/2}^{\rm calc1}$/s	$\lg T_{1/2}^{\rm calc2}$/s
nuclei in region I							
^{186}Po→^{182}Pb	8.501	$0^+ \to 0^+$	0	0.126	−4.469	−5.369	−4.641
^{190}Po→^{186}Pb	7.693	$0^+ \to 0^+$	0	0.201	−2.609	−3.307	−2.515
^{194}Po→^{190}Pb	6.987	$0^+ \to 0^+$	0	0.176	−0.407	−1.160	−0.293
^{196}Po→^{192}Pb	6.658	$0^+ \to 0^+$	0	0.172	0.754	−0.011	0.899
^{198}Po→^{194}Pb	6.310	$0^+ \to 0^+$	0	0.114	2.266	1.324	2.282
^{200}Po→^{196}Pb	5.981	$0^+ \to 0^+$	0	0.082	3.793	2.707	3.719
^{202}Po→^{198}Pb	5.700	$0^+ \to 0^+$	0	0.069	5.143	3.984	5.057
^{204}Po→^{200}Pb	5.485	$0^+ \to 0^+$	0	0.059	6.275	5.043	6.187
^{206}Po→^{202}Pb	5.327	$0^+ \to 0^+$	0	0.052	7.144	5.862	7.091
^{208}Po→^{204}Pb	5.216	$0^+ \to 0^+$	0	0.031	7.961	6.457	7.793
^{200}Rn→^{196}Po	7.043	$0^+ \to 0^+$	0	0.200	0.070	−0.629	0.099
^{202}Rn→^{198}Po	6.773	$0^+ \to 0^+$	0	0.159	1.090	0.291	1.083
^{204}Rn→^{200}Po	6.547	$0^+ \to 0^+$	0	0.128	2.012	1.120	1.987
^{206}Rn→^{202}Po	6.384	$0^+ \to 0^+$	0	0.105	2.737	1.757	2.715
^{208}Rn→^{204}Po	6.260	$0^+ \to 0^+$	0	0.074	3.367	2.236	3.309
^{210}Rn→^{206}Po	6.159	$0^+ \to 0^+$	0	0.048	3.954	2.631	3.861
^{212}Rn→^{208}Po	6.385	$0^+ \to 0^+$	0	0.029	3.157	1.616	3.093
^{204}Ra→^{200}Rn	7.637	$0^+ \to 0^+$	0	0.210	−1.222	−1.900	−1.253
^{208}Ra→^{204}Rn	7.273	$0^+ \to 0^+$	0	0.128	0.104	−0.789	0.039
^{214}Ra→^{210}Rn	7.273	$0^+ \to 0^+$	0	0.048	0.387	−0.933	0.543
^{212}Th→^{208}Ra	7.958	$0^+ \to 0^+$	0	0.163	−1.499	−2.287	−1.420
^{214}Th→^{210}Ra	7.827	$0^+ \to 0^+$	0	0.131	−1.060	−1.942	−0.869
^{216}U→^{212}Th	8.530	$0^+ \to 0^+$	0	0.078	−2.161	−3.266	−2.255
nuclei in regions II and III							
^{178}Pb→^{174}Hg	7.790	$0^+ \to 0^+$	0	0.380	−3.638	−4.059	−3.568
^{180}Pb→^{176}Hg	7.419	$0^+ \to 0^+$	0	0.220	−2.387	−3.045	−2.554
^{184}Pb→^{180}Hg	6.773	$0^+ \to 0^+$	0	0.160	−0.213	−1.011	−0.520
^{186}Pb→^{182}Hg	6.470	$0^+ \to 0^+$	0	0.099	1.072	0.069	0.560
^{188}Pb→^{184}Hg	6.109	$0^+ \to 0^+$	0	0.111	2.427	1.474	1.965
^{190}Pb→^{186}Hg	5.697	$0^+ \to 0^+$	0	0.107	4.245	3.273	3.763
^{192}Pb→^{188}Hg	5.221	$0^+ \to 0^+$	0	0.136	6.546	5.680	6.170
^{194}Pb→^{190}Hg	4.738	$0^+ \to 0^+$	0	0.019	10.234	8.511	9.002
^{210}Pb→^{206}Hg	3.793	$0^+ \to 0^+$	0	0.038	16.967	15.550	16.040
^{210}Po→^{206}Pb	5.408	$0^+ \to 0^+$	0	0.018	7.078	5.344	5.835
^{212}Po→^{208}Pb	8.954	$0^+ \to 0^+$	0	0.247	−6.531	−7.138	−6.666
^{214}Po→^{210}Pb	7.834	$0^+ \to 0^+$	0	0.268	−3.786	−4.358	−3.903
^{216}Po→^{212}Pb	6.907	$0^+ \to 0^+$	0	0.262	−0.839	−1.420	−0.981

Continued on next page

Table 1-continued from previous page

α transition	Q_α/MeV	$j_p^\pi \to j_d^\pi$	$l_{\min}$	P_α	$\lg T_{1/2}^{\rm expt}$/s	$\lg T_{1/2}^{\rm calc1}$/s	$\lg T_{1/2}^{\rm calc2}$/s
^{218}Po→^{214}Pb	6.115	$0^+ \to 0^+$	0	0.276	2.269	1.711	2.134
^{214}Rn→^{210}Po	9.208	$0^+ \to 0^+$	0	0.321	−6.569	−7.062	−6.606
^{216}Rn→^{212}Po	8.198	$0^+ \to 0^+$	0	0.497	−4.347	−4.650	−4.227
^{218}Rn→^{214}Po	7.263	$0^+ \to 0^+$	0	0.412	−1.472	−1.857	−1.464
^{220}Rn→^{216}Po	6.405	$0^+ \to 0^+$	0	0.388	1.745	1.334	1.698
^{216}Ra→^{212}Rn	9.526	$0^+ \to 0^+$	0	0.416	−6.740	−7.121	−6.682
^{218}Ra→^{214}Rn	8.546	$0^+ \to 0^+$	0	0.530	−4.599	−4.874	−4.481
^{216}Th→^{212}Ra	8.072	$0^+ \to 0^+$	0	0.073	−1.585	−2.724	−2.234
^{218}Th→^{214}Ra	9.849	$0^+ \to 0^+$	0	0.582	−6.932	−7.167	−6.744
^{220}Th→^{216} Ra	8.953	$0^+ \to 0^+$	0	0.604	−5.013	−5.232	−4.868
^{218}U→^{214}Th	8.775	$0^+ \to 0^+$	0	0.199	−3.260	−3.961	−3.470

Table 2. Same as Table 1, but for the favored α decay of the odd-A nuclei around the Z = 82, N = 126 shell closures. "()" represents uncertain spin and/or parity, and "#" represents values estimated from trends in neighboring nuclides with the same Z and N parities.

α transition	Q_α/MeV	$j_p^\pi \to j_d^\pi$	$l_{\min}$	P_α	$\lg T_{1/2}^{\rm expt}$/s	$\lg T_{1/2}^{\rm calc1}$/s	$\lg T_{1/2}^{\rm calc2}$/s
nuclei in region I							
^{195}Po→^{191}Pb	6.745	$(3/2^-) \to (3/2^-)$	0	0.100	0.692	−0.309	0.687
^{197}Po→^{193}Pb	6.405	$(3/2^-) \to (3/2^-)$	0	0.076	2.079	0.960	2.014
^{199}Po→^{195}Pb	6.075	$(3/2^-) \to 3/2^-$	0	0.047	3.639	2.314	3.434
^{201}Po→^{197}Pb	5.799	$3/2^- \to 3/2^-$	0	0.042	4.917	3.541	4.740
^{205}Po→^{201}Pb	5.325	$5/2^- \to 5/2^-$	0	0.050	7.185	5.887	7.309
^{207}Po→^{203}Pb	5.216	$5/2^- \to 5/2^-$	0	0.030	7.993	6.473	8.071
^{197}At→^{193}Bi	7.105	$(9/2^-) \to (9/2^-)$	0	0.155	−0.394	−1.205	−0.347
^{199}At→^{195}Bi	6.778	$9/2^{(-)} \to 9/2^{(-)}$	0	0.106	0.894	−0.080	0.841
^{201}At→^{197}Bi	6.473	$(9/2^-) \to (9/2^-)$	0	0.095	2.076	1.053	2.048
^{203}At→^{199}Bi	6.210	$9/2^- \to 9/2^-$	0	0.087	3.152	2.091	3.176
^{205}At→^{201}Bi	6.019	$9/2^- \to 9/2^-$	0	0.040	4.299	2.901	4.101
^{207}At→^{203}Bi	5.873	$9/2^- \to 9/2^-$	0	0.054	4.814	3.549	4.903
^{209}At→^{205}Bi	5.757	$9/2^- \to 9/2^-$	0	0.025	5.672	4.068	5.666
^{211}At→^{207}Bi	5.983	$9/2^- \to 9/2^-$	0	0.014	4.793	2.945	5.144
^{195}Rn→^{191}Po	7.694	$3/2^- \to (3/2^-)$	0	0.322	−2.155	−2.647	−1.991
^{197}Rn→^{193}Po	7.410	$(3/2^-) \to (3/2^-)$	0	0.289	−1.268	−1.807	−1.099
^{203}Rn→^{199}Po	6.629	$3/2^-\# \to (3/2^-)$	0	0.101	1.818	0.825	1.745
^{207}Rn→^{203}Po	6.251	$5/2^- \to 5/2^-$	0	0.076	3.417	2.299	3.458
^{209}Rn→^{205}Po	6.155	$5/2^- \to 5/2^-$	0	0.048	4.000	2.683	4.037
^{199}Fr→^{195}At	7.816	$1/2^+\# \to 1/2^+$	0	0.298	−2.180	−2.706	−2.063
^{201}Fr→^{197}At	7.519	$(9/2^-) \to (9/2^-)$	0	0.231	−1.202	−1.839	−1.130
^{203}Fr→^{199}At	7.274	$9/2^- \to 9/2^{(-)}$	0	0.146	−0.260	−1.096	−0.312
^{205}Fr→^{201}At	7.054	$9/2^- \to (9/2^-)$	0	0.112	0.582	−0.370	0.507
^{207}Fr→^{203}At	6.894	$9/2^- \to 9/2^-$	0	0.096	1.190	0.171	1.167
^{209}Fr→^{205}At	6.777	$9/2^- \to 9/2^-$	0	0.064	1.753	0.561	1.719

Continued on next page

Table 2-continued from previous page

α transition	Q_α/MeV	$j_p^\pi \to j_d^\pi$	$l_{\min}$	P_α	$\lg T_{1/2}^{\rm expt}$/s	$\lg T_{1/2}^{\rm calc1}$/s	$\lg T_{1/2}^{\rm calc2}$/s
^{211}Fr$\to^{207}$At	6.662	$9/2^- \to 9/2^-$	0	0.043	2.328	0.958	2.379
^{213}Fr$\to^{209}$At	6.905	$9/2^- \to 9/2^-$	0	0.028	1.535	−0.014	2.185
^{203}Ra$\to^{199}$Rn	7.735	$(3/2^-) \to (3/2^-)$	0	0.185	−1.444	−2.177	−1.509
^{209}Ra$\to^{205}$Rn	7.143	$5/2^- \to 5/2^-$	0	0.092	0.673	−0.363	0.632
^{205}Ac$\to^{201}$Fr	8.096	$9/2^-\# \to (9/2^-)$	0	0.016	−1.097	−2.904	−2.261
^{207}Ac$\to^{203}$Fr	7.849	$9/2^-\# \to 9/2^-$	0	0.197	−1.509	−2.214	−1.477
^{211}Ac$\to^{207}$Fr	7.619	$9/2^- \to 9/2^-$	0	0.117	−0.672	−1.605	−0.582
^{213}Pa$\to^{209}$Ac	8.395	$9/2^-\# \to (9/2^-)$	0	0.094	−2.155	−3.184	−2.263
^{215}Pa$\to^{211}$Ac	8.235	$9/2^-\# \to 9/2^-$	0	0.116	−1.854	−2.791	−1.591
nuclei in regions II and III							
^{177}Tl$\to^{173}$Au	7.066	$(1/2^+) \to (1/2^+)$	0	0.223	−1.609	−0.652	−1.821
^{179}Tl$\to^{175}$Au	6.705	$1/2^+ \to 1/2^+$	0	0.188	−0.356	−0.726	−0.634
^{213}Po$\to^{209}$Pb	8.536	$9/2^+ \to 9/2^+$	0	0.177	−5.431	−0.752	−5.641
^{215}Po$\to^{211}$Pb	7.527	$9/2^+ \to 9/2^+$	0	0.193	−2.750	−0.714	−2.942
^{219}Po$\to^{215}$Pb	5.916	$9/2^+\# \to 9/2^+\#$	0	0.179	3.340	−0.747	3.082
^{213}At$\to^{209}$Bi	9.254	$9/2^- \to 9/2^-$	0	0.274	−6.903	−0.562	−6.925
^{215}At$\to^{211}$Bi	8.178	$9/2^- \to 9/2^-$	0	0.112	−4.000	−0.951	−4.438
^{217}At$\to^{213}$Bi	7.202	$9/2^- \to 9/2^-$	0	0.273	−1.487	−0.564	−1.564
^{219}At$\to^{215}$Bi	6.342	$(9/2^-) \to (9/2^-)$	0	0.242	1.777	−0.616	1.623
^{215}Rn$\to^{211}$Po	8.839	$9/2^+ \to 9/2^+$	0	0.249	−5.638	−0.604	−5.728
^{217}Rn$\to^{213}$Po	7.888	$9/2^+ \to 9/2^+$	0	0.296	−3.268	−0.529	−3.316
^{215}Fr$\to^{211}$At	9.541	$9/2^- \to 9/2^-$	0	0.405	−7.066	−0.393	−6.937
^{217}Fr$\to^{213}$At	8.470	$9/2^- \to 9/2^-$	0	0.572	−4.775	−0.243	−4.538
^{219}Fr$\to^{215}$At	7.449	$9/2^- \to 9/2^-$	0	0.395	−1.699	−0.403	−1.662
^{2137}Ra$\to^{213}$Rn	9.161	$(9/2^+) \to 9/2^+\#$	0	0.286	−5.788	−0.544	−5.845
^{215}Ac$\to^{211}$Fr	7.746	$9/2^- \to 9/2^-$	0	0.046	−0.770	−1.337	−1.536
^{217}Ac$\to^{213}$Fr	9.832	$9/2^- \to 9/2^-$	0	0.534	−7.161	−0.272	−6.929
^{219}Ac$\to^{215}$Fr	8.827	$9/2^- \to 9/2^-$	0	0.480	−4.928	−0.319	−4.800
^{219}Th$\to^{215}$Ra	9.511	$9/2^+\# \to 9/2^+\#$	0	0.312	−5.991	−0.506	−6.034
^{217}Pa$\to^{213}$Ac	8.488	$9/2^-\# \to 9/2^-\#$	0	0.082	−2.458	−1.086	−2.975
^{219}Pa$\to^{215}$ Ac	10.084	$9/2^- \to 9/2^-$	0	0.826	−7.276	−0.083	−6.871
^{221}Pa$\to^{217}$Ac	9.251	$9/2^- \to 9/2^-$	0	0.415	−5.229	−0.382	−5.193
^{221}U$\to^{217}$Th	9.889	$(9/2^+) \to 9/2^+\#$	0	0.312	−6.180	−0.506	−6.246

dots in the right sides of Figs. 2 and 3 deviate significantly from the fitted line. Careful analysis of the right side of Fig. 2 reveals an interesting phenomenon: the P_α values of some odd-Z nuclei are even larger than the ones of most even–even nuclei, i.e., P_α 0.572 for ^{217}Fr, 0.534 for ^{217}Ac, and 0.826 for ^{219}Pa. Theoretically, for the odd-A and odd–odd nuclei, owing to the Pauli-blocking effect, the unpaired nucleon (s) would lead to α particle formation suppression; thus, the P_α of odd-A nuclei should not be extremely large. In response to above phenomenon presented in the right side of Fig. 2, we note that the neutron numbers, N, of ^{217}Fr, ^{217}Ac, and ^{219}Pa are 130, 128, and 128, respectively, which are near the magic number, N = 126. Recent studies have shown that the P_α values decrease with increasing neutron number until the shell closure at N = 126, and then sharply increase with N, suggesting the important influence of the shell effect on the α particle preformation process in the parent nuclei [62,

Table 3. Same as Tables 1 and 2, but for the unfavored α decay of the odd-A nuclei around the doubly magic core at $Z = 82$, $N = 126$.

α transition	Q_α/MeV	$j_p^\pi \to j_d^\pi$	$l_{\min}$	P_α	$\lg T_{1/2}^{\rm expt}$/s	$\lg T_{1/2}^{\rm calc1}$/s	$\lg T_{1/2}^{\rm calc2}$/s
nuclei in region I							
^{209}Bi→^{205}Tl	3.138	$9/2^- \to 1/2^+$	5	0.001	26.802	23.934	25.999
^{189}Po→^{185}Pb	7.694	$(5/2^-) \to 3/2^-$	2	0.158	−2.420	−3.223	−2.383
^{203}Po→^{199}Pb	5.496	$5/2^- \to 3/2^-$	2	0.062	6.294	5.085	6.353
^{205}Rn→^{201}Po	6.386	$5/2^-\# \to 3/2^-\#$	2	0.100	2.837	1.840	2.843
^{207}Ra→^{203}Rn	7.269	$1/2^- \to 5/2^-$	2	0.129	0.205	−0.683	0.157
^{213}Ra→^{209}Rn	6.862	$(1/2^-) \to 5/2^{(-)}$	2	0.022	2.309	0.641	2.194
^{215}Th→^{211}Ra	7.665	$1/2^-\# \to 5/2^-\#$	2	0.034	0.079	−1.387	0.074
nuclei in regions II and III							
^{187}Pb→^{183}Hg	6.393	$3/2^- \to 1/2^-$	2	0.016	2.203	0.406	2.471
^{189}Pb→^{185}Hg	5.915	$3/2^- \to 1/2^-$	2	0.024	3.989	2.375	4.440
^{213}Bi→^{209}Ti	5.988	$9/2^- \to 1/2^+$	5	0.001	5.116	2.256	5.214
^{213}Rn→^{209}Po	8.245	$9/2^+\# \to 1/2^-$	5	0.002	−1.710	−4.444	−1.486
^{219}Rn→^{215}Po	6.946	$5/2^+ \to 9/2^+$	2	0.048	0.598	−0.720	0.794
^{221}Rn→^{217}Po	6.162	$7/2^+ \to (9/2^+)$	2	0.040	3.844	2.442	3.835
^{215}Ra→^{211}Rn	8.864	$9/2^+\# \to 1/2^-$	5	0.003	−2.777	−5.364	−2.916
^{219}Ra→^{215}Rn	8.138	$(7/2^+) \to 9/2^+$	2	0.018	−2.000	−3.754	−2.274
^{217}Th→^{213} Ra	9.435	$9/2^+\# \to 1/2^-$	5	0.004	−3.607	−6.048	−3.828

Table 4. Same as Tables 1 and 2, but for the favored α decay of the doubly-odd nuclei.

α transition	Q_α/MeV	$j_p^\pi \to j_d^\pi$	$l_{\min}$	P_α	$\lg T_{1/2}^{\rm expt}$/s	$\lg T_{1/2}^{\rm calc1}$/s	$\lg T_{1/2}^{\rm calc2}$/s
nuclei in region I							
^{192}At→^{188}Bi	7.696	$3^+\# \to 3^+\#$	0	0.115	−1.939	−2.957	−2.019
^{200}At→^{196}Bi	6.596	$(3^+) \to (3^+)$	0	0.059	1.917	0.594	1.823
^{202}At→^{198}Bi	6.353	$3^{(+)} \to 3^{(+)}$	0	0.045	3.161	1.511	2.857
^{204}At→^{200}Bi	6.071	$7^+ \to 7^+$	0	0.031	4.156	2.689	4.198
^{206}At→^{202}Bi	5.886	$(5)^+ \to 5^{(+\#)}$	0	0.017	5.306	3.506	5.279
^{208}At→^{204}Bi	5.751	$6^+ \to 6^+$	0	0.003	6.023	4.114	6.667
^{200}Fr→^{196}At	7.615	$(3^+) \to (3^+)$	0	0.134	−1.323	−2.113	−1.240
^{204}Fr→^{200}At	7.170	$3^+ \to (3^+)$	0	0.087	0.260	−0.764	0.295
^{206}Fr→^{202}At	6.924	$3^+ \to 3^{(+)}$	0	0.064	1.258	0.084	1.279
^{208}Fr→^{204}At	6.784	$7^+ \to 7^+$	0	0.040	1.821	0.555	1.950
^{206}Ac→^{202}Fr	7.959	$(3^+) \to 3^+$	0	0.129	−1.602	−2.528	−1.640
nuclei in regions II and III							
^{214}At→^{210}Bi	8.987	$1^- \to 1^-$	0	0.186	−6.253	−6.912	−6.182
^{216}At→^{212}Bi	7.950	$1^{(-)} \to 1^{(-)}$	0	0.218	−3.523	−4.336	−3.674
^{218}At→^{214}Bi	6.874	$1^-\# \to 1^-$	0	0.249	0.176	−0.910	−0.307
^{216}Fr→^{212}At	9.175	$(1^-) \to (1^-)$	0	0.218	−6.155	−6.685	−6.022
^{218}Fr→^{214}At	8.014	$1^- \to 1^-$	0	0.270	−3.000	−3.791	−3.223
^{218}Ac→^{214}Fr	9.374	$1^-\# \to (1^-)$	0	0.249	−6.000	−6.487	−5.884
^{220}Pa→^{216}Ac	9.651	$1^-\# \to (1^-)$	0	0.281	−6.108	−6.471	−5.920

Table 5. Same as Tables 1 and 2, but for the unfavored α decay of the doubly-odd nuclei.

α transition	Q_α/MeV	$j_p^\pi \to j_d^\pi$	$l_{\min}$	P_α	$\lg T_{1/2}^{\rm expt}$/s	$\lg T_{1/2}^{\rm calc1}$/s	$\lg T_{1/2}^{\rm calc2}$/s
nuclei in region I							
^{186}Bi→^{182}Tl	7.757	$(3^+) \to (2^-)$	1	0.012	−1.830	−3.749	−2.092
^{190}Bi→^{186}Tl	6.862	$(3^+) \to (2^-)$	1	0.012	0.912	0.688	3.704
^{192}Bi→^{188}Tl	6.381	$(3^+) \to (2^-)$	1	0.020	2.442	2.478	2.852
^{194}Bi→^{190}Tl	5.918	$(3^+) \to (2^-)$	1	0.023	4.313	4.420	2.697
^{210}At→^{206}Bi	5.631	$(5)^+ \to (6)^+$	2	0.003	7.221	6.687	6.125
^{210}Fr→^{206}At	6.672	$6^+ \to (5)^+$	2	0.038	2.427	2.755	2.019
^{212}Fr→^{208}At	6.529	$5^+ \to 6^+$	2	0.012	3.444	3.442	3.626
^{212}Pa→^{208}Ac	8.415	$7^+\# \to (3^+)$	4	0.021	−2.125	−3.794	−2.116
nuclei in regions II and III							
^{210}Bi→^{206}Tl	5.037	$1^- \to 0^-$	2	2.330E-05	11.616	10.343	21.455
^{212}Bi→^{208}Tl	6.207	$1^{(-)} \to 5^+$	5	0.002	4.005	4.171	7.326
^{214}Bi→^{210}Tl	5.621	$1^- \to 5^+\#$	5	0.002	6.753	6.667	7.478
^{212}At→^{208}Bi	7.817	$(1^-) \to 5^+$	5	0.001	−0.503	−0.719	9.542
^{214}Fr→^{210}At	8.588	$(1^-) \to (5)^+$	5	0.002	−2.286	−2.359	7.413
^{216}Ac→^{212}Fr	9.235	$(1^-) \to 5^+$	5	0.003	−3.357	−3.423	6.596

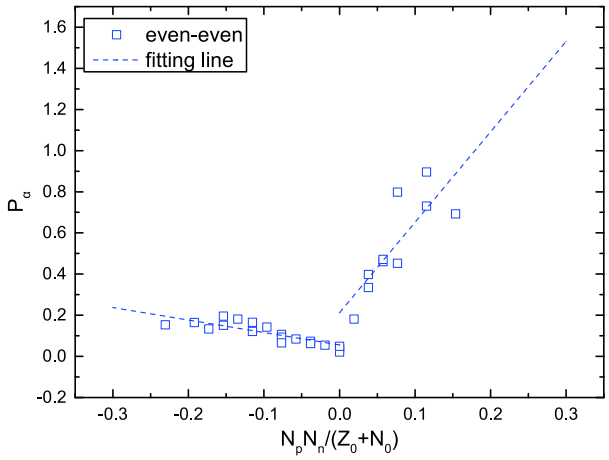

Fig. 4. (color online) α preformation factors P_α of the even–even nuclei around the Z_0 = 82 and N_0 = 126 shell closures as a function of $\frac{N_pN_n}{N_0+Z_0}$, where P_α are obtained by Eq. (14). The blue open squares denote the even–even nuclei around the shell closures, and the blue dashed lines are the fittings of P_α.

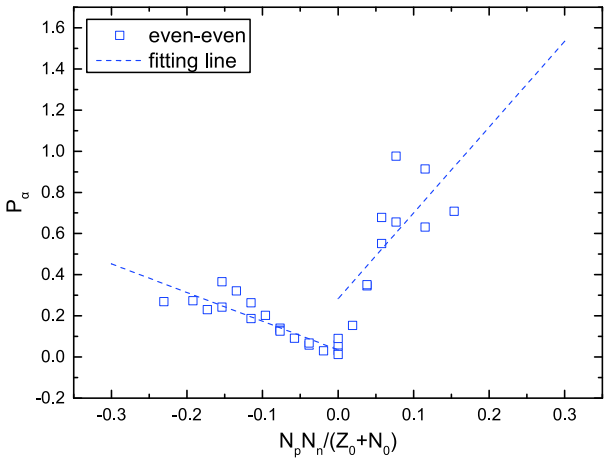

Fig. 5. (color online) Same as Fig. 4, but the α preformation factors, P_α, are calculated by Eq. (15).

63]. As we can see from the right side in Fig. 3, there are seven red dots for favored odd –odd nuclei decay; however, we can find that five of them have uncertain spin or parity from Table 4 i.e., ^{216}At and ^{216}Fr. Hence, the inaccuracy of the minimum angular momentum taken away by the α particle ($l_{\min}$) will, in turn, affect the P_α values extracted from the ratio of the calculated decay half-life to the experimental one.

In 2018, based on the single-particle energy spectra obtained by the relativistic Hartree –Bogoliubov mean field model [64], Sun and Zhang defined the microscopic valence nucleon (holes) numbers (Ω_π, Ω_ν) and proposed two different formulas to calculate P_α, which can be expressed as [65]

$$P_\alpha = a\Omega_\pi\Omega_\nu\left\{1+b\exp\left[-\frac{(\lambda_\pi-\lambda_\nu)^2}{2\sigma^2}\right]\right\}, \quad (14)$$

$$P_\alpha = a_{nn,nh}\Omega_\pi\Omega_\nu. \quad (15)$$

Here, parameters a, b, and σ in Eq. (14) as well as $a_{nn,nh}$ in Eq. (15) correspond to the valence proton–neutron interaction strength.

In their study, using the above formulas, they systematically investigated the α decay preformation factors, P_α, for even–even polonium, radon, radium, and thorium isotopes. Based on the calculated results of their study, we plot P_α as a function of $\frac{N_pN_n}{Z_0+N_0}$ in Figs. 4 and 5. In these figures, the blue opened squares represent the even–even nuclei extracted from the study of Sun and Zhang, which are located around the shell closures, and the blue dashed lines represent the fittings of the P_α. As we can see from these figures, like Fig. 1, for the case of even–even nuclei, the P_α obtained by Eq. (14) and Eq. (15) also have a noticeable linear relationship with $\frac{N_pN_n}{Z_0+N_0}$. This phenomenon further suggests that this linear relationship is not model-dependent. Furthermore, for the case of unfavored α decay, from Figs. 2 and 3, we find that the values of P_α are relatively small relative to those for the favored α decay. The reasons may be the influence of the centrifugal potential, which reduces the α decay width, or the nuclear structure configuration changes. Combining with the analysis results of Figs. 1-3, we suspect the linear relationship between P_α and N_pN_n for all kinds of nuclei may be related to the effect of the valence proton–neutron interaction around shell closures. In order to more deeply study the relationship between α preformation factors P_α and N_pN_n, all the cases of P_α can be obtained by the linear relationship.

$$P_\alpha = a\frac{N_pN_n}{Z_0+N_0}+b. \tag{16}$$

Here, a and b are adjustable parameters, which are extracted from the fittings of Figs. 1-3 and listed in Table 6. In theory, combining these parameters and Eq. (15), one can obtain the fitted P_α.

We systematically calculate the α decay half-lives of the 152 nuclei using the GLDM. All the numerical results are listed in Tables 1- 5. In these tables, the first five columns denote the α transition, α decay energy Q_α as taken from the latest evaluated atomic mass table, AME2016 [60, 61], spin-parity transformation ($j_p^\pi \to j_d^\pi$), minimum orbital angular momentum $l_{\min}$ taken away by the α particle, and α preformation factor, respectively. The sixth column denotes the logarithmic form of the experimental α decay half-life denoted as $\lg T_{1/2}^{\exp}$. The last two columns denote the logarithmic form of the calculated α decay half-life using the GLDM without considering P_α and with fitting P_α calculated by Eq. (15), which are denoted as $\lg T_{1/2}^{\rm calc1}$ and $\lg T_{1/2}^{\rm calc2}$, respectively. Simultaneously, each table is divided into two parts: region I and regions II and III. As can be seen from Tables 1-5, relative to $\lg T_{1/2}^{\rm calc1}$, $\lg T_{1/2}^{\rm calc2}$ can better reproduce the experimental data. More intuitively, we calculate the standard deviation, $\sigma=\sqrt{\sum(\log_{10}T_{1/2}^{\rm calc}-\log_{10}T_{1/2}^{\exp})^2/n}$, between the calculated α decay half-lives and the experimental data. The calculated results are summarized in Table 7. In this table, σ_1 and σ_2 represent the standard deviations between $T_{1/2}^{\rm calc1}$, $T_{1/2}^{\rm calc2}$ and $T_{1/2}^{\exp}$, respectively. As we can see from Table 7, it is noticeable that for all the kinds of nuclei, the values of σ_1 are much larger than the values of σ_2. The maximum value of σ_2 is only 0.40, which suggests that the calculated α decay half-lives using the GLDM with the fitting of P_α calculated by Eq. (15) can better reproduce the experimental data. Moreover, for more clearly indicating the agreement between the calculations using the GLDM with the fitting P_α and the experimental data, we plot the logarithm deviation between the calculated results and experimental data for all kinds of nuclei in Figs. 6(a)-6(c). In Figs. 6(a)-6(c), the opened blue circles denote the logarithm deviation between the calculated results and the experimental data for the cases of favored α decay for all the kinds of nuclei. The red circles in Figs. 6(b)- 6(c) denote the cases of unfavored α decay for the odd-A and odd–odd nuclei, respectively. One can see from Figs. 6(a)-6(c), the values of $\log_{10}T_{1/2}^{\rm cal}-\log_{10}T_{1/2}^{\exp}$ are basically between -0.4 and 0.4. This indicates that the GLDM with the fitting of P_α can be treated as a useful tool to study the α decay half-lives of the nuclei around the $Z=82$, $N=126$ shell closures.

Table 6. Fitted parameters of Eq. (16).

region	favored decay		unfavored decay	
	a	b	a	b
even–even nuclei				
I	−0.66547	0.03339	–	–
II, III	1.8334	0.25035	–	–
odd-A nuclei				
I	−0.65688	0.00632	−0.67342	0.00862
II, III	0.64805	0.26947	0.2559	−0.00382
doubly-odd nuclei				
I	−0.48781	−0.01831	−0.10994	0.00988
II, III	1.0972	0.13849	0.09388	-1.34923×10^{-4}

4 Summary

Table 7. Standard deviation σ between the calculated α decay half-lives and the experimental ones.

nuclei	favored decay		unfavored decay	
	σ_1	σ_2	σ_1	σ_2
even–even nuclei	0.947	0.350	–	–
odd – A nuclei	0.978	0.262	1.90	0.272
doubly odd nuclei	1.145	0.227	2.494	0.400

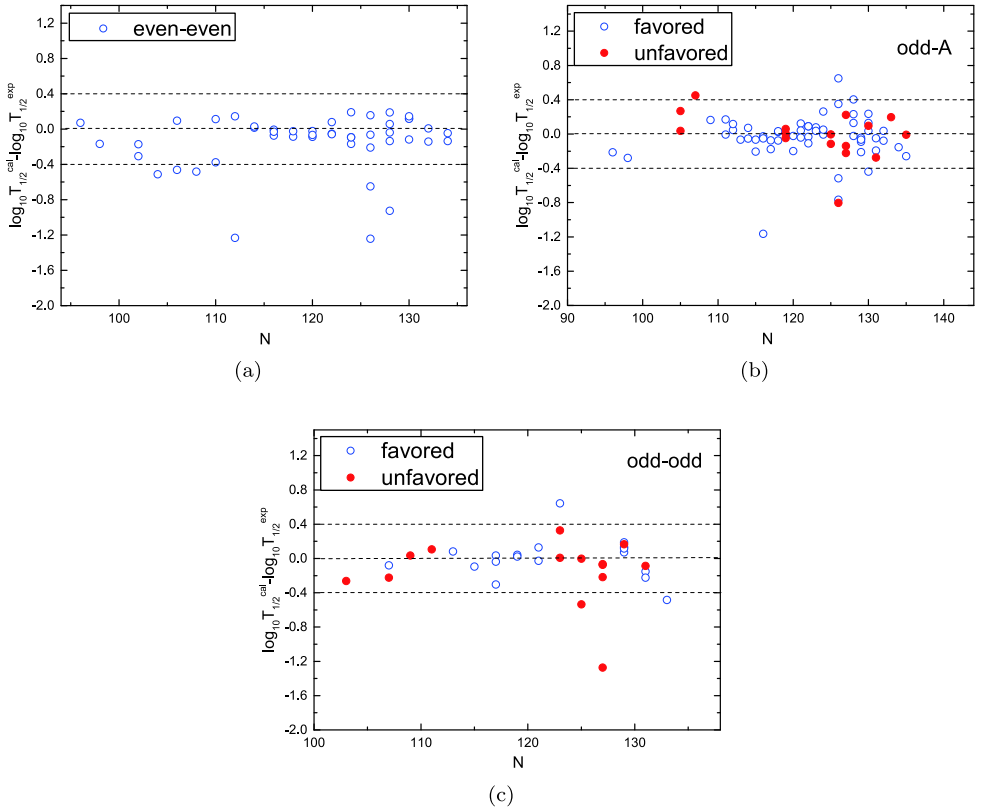

Fig. 6. (color online) Deviations of the logarithmic form of the α decay half-lives between the calculations using the GLDM with the fitting of P_α calculated by Eq. (16) and the experimental data as a function of the neutron number.

In summary, using the GLDM, we systematically study the α decay half-lives and the preformation factors of 152 nuclei around $Z = 82$, $N = 126$ closed shells. It is found that the preformation factors are linearly related to N_pN_n and the calculated half-lives can reproduce the experimental data well. Meanwhile, the linear relationship between N_pN_n and the preformation factors calculated by two different formulas by defining the concept of the microscopic valence nucleon (hole) number still exists. Combining with the study of Seif *et al*. and our previous studies, we consider that the linear relationship between P_α and N_pN_n around the $Z = 82$, $N = 126$ shell closures is model-independent and that the valance proton–neutron interaction may be important to the α particle preformation.

We would like to thank X. -D. Sun, J. -G. Deng, J. -H. Cheng, and J. -L. Chen for useful discussion.

References

1 D. S. Delion, S. Peltonen, and J. Suhonen, Phys. Rev. C, **73**: 014315 (2006)
2 P. R. Chowdhury, C. Samanta, and D. N. Basu, Phys. Rev. C, **73**: 014612 (2006)
3 W. M. Seif, Phys. Rev. C, **74**: 034302 (2006)
4 D. N. Basu, J. Phys. G: Nucl. Part. Phys., **30**: B35 (2004)
5 R. W. Gurney and E. U. Condon, Nature(London), **122**: 439 (1928)
6 G. Gamow, Z. Phys., **51**: 204 (1928)
7 C. Qi, Reviews in Physics, **1**: 77 (2016)
8 H. F. Zhang and G. Royer, Phys. Rev. C, **77**: 054318 (2008)
9 W. M. Seif, M. M. Botros, and A. I. Refaie, Phys. Rev. C, **92**: 044302 (2015)
10 C. Xu, G. Röpke, P. Schuck *et al*., Phys. Rev. C, **95**: 061306(R) (2017)
11 K. Varga, R. G. Lovas, and R. J. Liotta, Phys. Rev. Lett., **69**: 37 (1992)
12 G. Dodig-Crnković, F. Janouch, R. Liotta *et al*., Nucl. Phys. A, **444**: 419 (1985)
13 I. Tonozuka and A. Arima, Nucl. Phys. A, **323**: 45 (1979)
14 G. Dodig-Crnković, F. Janouch, and R. Liotta, Nucl. Phys. A, **501**: 533 (1989)
15 K. Varga, R. Lovas, and R. Liotta, Nucl. Phys. A, **550**: 421 (1992)
16 G. Röpke, P. Schuck, Y. Funaki *et al*., Phys. Rev. C, **90**: 034304 (2014)
17 C. Xu, Z. Z. Ren, G. Röpke *et al*., Phys. Rev. C, **93**: 011306(R) (2016)
18 C. Xu and Z. Ren, Nucl. Phys. A, **760**: 303 (2005)
19 S. M. S. Ahmed, R. Yahaya, S. Radiman *et al*., J. Phys. G: Nucl. Part. Phys., **40**: 065105 (2013)
20 D. Deng, Z. Ren, D. Ni *et al*., J. Phys. G: Nucl. Part. Phys., **42**: 075106 (2015)
21 D. M. Deng and Z. Z. Ren, Phys. Rev. C, **93**: 044326 (2016)

22 S. M. S. Ahmed, Nucl. Phys. A, **962**: 103 (2017)
23 H. F. Zhang, G. Royer, and J. Q. Li, Phys. Rev. C, **84**: 027303 (2011)
24 G. L. Zhang, X. Y. Le, and H. Q. Zhang, Phys. Rev. C, **80**: 064325 (2009)
25 Y. B. Qian and Z. Z. Ren, Sci. Chin. Phys., Mech. Astron., **56**: 1520 (2013)
26 S. M. S. Ahmed, R. Yahaya, and S. Radiman, Rom. Rep. Phys., **65**: 1281 (2013)
27 W. M. Seif, J. Phys. G: Nucl. Part. Phys., **40**: 105102 (2013)
28 A. N. Andreyev, M. Huyse, P. Van Duppen *et al*., Phys. Rev. Lett., **110**: 242502 (2013)
29 M. Ismail and A. Adel, Phys. Rev. C, **89**: 034617 (2014)
30 J. R. Stone, K. Morita, P. A. M. Guichon *et al*., Phys. Rev. C, **100**: 044302 (2019)
31 C. Qi, R. Liotta and R. Wyss, Prog. Part. Nucl. Phys, **105**: 214 (2019)
32 R. F. Casten and N. V. Zamfir, Phys. Rev. Lett., **70**: 402 (1993)
33 Y. M. Zhao, A. Arima, and R. F. Casten, Phys. Rev. C, **63**: 067302 (2001)
34 M. Saha and S. Sen, Phys. Rev. C, **46**: R1587 (1992)
35 B. Buck, A. C. Merchant, and S. M. Perez, Phys. Rev. Lett., **94**: 202501 (2005)
36 R. F. Casten, Phys. Rev. C, **33**: 1819 (1986)
37 W. M. Seif, M. Shalaby, and M. F. Alrakshy, Phys. Rev. C, **84**: 064608 (2011)
38 X. D. Sun, P. Guo, and X. H. Li, Phys. Rev. C, **94**: 024338 (2016)
39 J. G. Deng, J. C. Zhao, D. Xiang *et al*., Phys. Rev. C, **96**: 024318 (2017)
40 J. G. Deng, J. C. Zhao, P. C. Chu *et al*., Phys. Rev. C, **97**: 044322 (2018)
41 S. A. Gurvitz and G. Kalbermann, Phys. Rev. Lett., **59**: 262 (1987)
42 S. A. Gurvitz, P. B. Semmes, W. Nazarewicz *et al*., Phys. Rev. A, **69**: 042705 (2004)
43 J. Bocki, J. Randrup, W. wiatecki *et al*., Ann. Phys.(N.Y.), **105**: 427 (1977)
44 G. Royer, J. Phys. G: Nucl. Part. Phys., **26**: 1149 (2000)
45 G. Royer and R. Moustabchir, Nucl. Phys. A, **683**: 182 (2001)
46 H. F. Zhang, W. Zuo, J. Q. Li *et al*., Phys. Rev. C, **74**: 017304 (2006)
47 G. Royer and B. Remaud, Nucl. Phys. A, **444**: 477 (1985)
48 X. J. Bao, H. F. Zhang, B. S. Hu *et al*., J. Phys. G: Nucl. Part. Phys., **39**: 095103 (2012)
49 X. J. Bao, H. F. Zhang, G. Royer *et al*., Nucl. Phys. A, **906**: 1 (2013)
50 J. M. Dong, W. Zuo, J. Z. Gu *et al*., Phys. Rev. C, **81**: 064309 (2010)
51 W. D. Myers and W. J. Świątecki, Phys. Rev. C, **62**: 044610 (2000)
52 C. Xu and Z. Z. Ren, Phys. Rev. C, **69**: 024614 (2004)
53 V. Y. Denisov and A. A. Khudenko, Phys. Rev. C, **82**: 059901(E) (2010)
54 A. de Shalit and M. Goldhaber, Phys. Rev., **92**: 1211 (1953)
55 I. Talmi, Rev. Mod. Phys., **34**: 704 (1963)
56 P. Federman, S. Pittel, and R. Campos, Phys. Lett. B, **82**: 9 (1979)
57 R. F. Casten, Phys. Rev. Lett., **54**: 1991 (1985)
58 R. F. Casten, D. S. Brenner, and P. E. Haustein, Phys. Rev. Lett., **58**: 658 (1987)
59 G. Audi, F. G. Kondev, M. Wang *et al*., Chin. Phys. C, **41**: 030001 (2017)
60 M. Wang, G. Audi, F. G. Kondev *et al*., Chin. Phys. C, **47**: 030003 (2017)
61 W. Huang, G. Audi, M. Wang *et al*., Chin. Phys. C, **41**: 030002 (2017)
62 G. L. Zhang, X. Y. Le, and H. Q. Zhang, Nucl. Phys. A, **823**: 16 (2009)
63 Y. W. Zhao, S. Q. Guo, and H. F. Zhang, Chin. Phys. C, **42**: 074103 (2018)
64 W. H. Long, H. Sagawa, N. V. Giai *et al*., Phys. Rev. C, **76**: 034314 (2007)
65 X. D. Sun and H. F. Zhang, J. Phys. G: Nucl. Part. Phys., **45**: 075106 (2018)